### Title
Shikimic acid ozonolysis kinetics of the transition from liquid aqueous solution to highly viscous glass




### Journal
Physical Chemistry Chemical Physics, 17(46)

### ISSN
0956-5000



### Authors
Steimer, Sarah S
Berkemeier, Thomas
Gilgen, Anina
et al.



### Publication Date
2015-12-14

### DOI
10.1039/c5cp04544d

Peer reviewed

PCCP

PAPER

View Article Online
View Journal | View Issue



Cite this: *Phys. Chem. Chem. Phys.*, 2015, **17**, 31101

# Shikimic acid ozonolysis kinetics of the transition from liquid aqueous solution to highly viscous glass

Sarah S. Steimer,†[ab] Thomas Berkemeier,[c] Anina Gilgen,[b] Ulrich K. Krieger,[b] Thomas Peter,[b] Manabu Shiraiwa[c] and Markus Ammann*[a]

Received 31st July 2015,
Accepted 16th October 2015

DOI: 10.1039/c5cp04544d

www.rsc.org/pccp

Ageing of particulate organic matter affects the composition and properties of atmospheric aerosol particles. Driven by temperature and humidity, the organic fraction can vary its physical state between liquid and amorphous solid, or rarely even crystalline. These transitions can influence the reaction kinetics due to limitations of mass transport in such (semi-) solid states, which in turn may influence the chemical ageing of particles containing such compounds. We have used coated wall flow tube experiments to investigate the reaction kinetics of the ozonolysis of shikimic acid, which serves as a proxy for oxygenated, water-soluble organic matter and can form a glass at room temperature. Particular attention was paid to how the presence of water influences the reaction, since it acts a plasticiser and thereby induces changes in the physical state. We analysed the results by means of a traditional resistor model, which assumes steady-state conditions. The ozonolysis rate of shikimic acid is strongly increased in the presence of water, a fact we attribute to the increased transport of $O_3$ and shikimic acid through the condensed phase at lower viscosities. The analysis using the resistor model suggests that the system undergoes both surface and bulk reaction. The second-order rate coefficient of the bulk reaction is 3.7 (+1.5/−3.2) × $10^3$ L $mol^{-1}$ $s^{-1}$. At low humidity and long timescales, the resistor model fails to describe the measurements appropriately. The persistent $O_3$ uptake at very low humidity suggests contribution of a self-reaction of $O_3$ on the surface.

## Introduction

Organic matter (OM) constitutes a significant fraction of atmospheric aerosol mass.[1,2] Aerosols undergo physical and chemical ageing in the atmosphere, which can change their properties such as absorptivity,[3] hygroscopicity[4] and toxicity.[5,6] OM in aerosols has often been assumed to be well mixed, with respect to both gas–particle partitioning[7,8] and reactions in the condensed phase (subsequently termed "bulk", in contrast to the particle's surface region). This provides the basis for theoretical descriptions of secondary organic aerosols (SOA). However, recent studies of glass transition temperatures,[9] particle bouncing behaviour,[10] evaporation,[11–13] thermal desorption[14] and response to physical deformation[15] show that OM can adopt a semi-solid or amorphous solid (glassy) state under environmental conditions. Starting from aqueous organic liquids which exist in the atmosphere at high RH, the self-diffusion coefficient (of the organic solute) can decrease with decreasing RH from around $10^{-8}$ $cm^2$ $s^{-1}$ to less than $10^{-20}$ $cm^2$ $s^{-1}$.[15] The change in diffusivity of small guest molecules is expected to be much smaller, for example, from $10^{-5}$ $cm^2$ $s^{-1}$ to about $10^{-10}$ to $10^{-12}$ $cm^2$ $s^{-1}$ for water at room temperature.[9,16] These changes in diffusion coefficients have important implications for mass transport based processes such as gas–particle partitioning.[17] A study by Abramson *et al.* on evaporation from α-pinene-derived SOA shows that pyrene present during SOA formation gets trapped and despite its relatively high volatility evaporates only slowly due to slow diffusion within the bulk.[12] Another example of non-equilibrium formation and growth of SOA is presented in a study by Perraud *et al.*, who show that organic nitrates were buried in α-pinene-derived SOA instead of following equilibrium partitioning.[18] As diffusivity influences the supply of reactants, changes in the physical state have potential to change reaction rates and kinetic regimes, which will in turn influence aerosol properties and lifetime.[19] First investigations of this phenomenon were performed by Shiraiwa *et al.* in a study on the

[a] *Paul Scherrer Institute, Laboratory of Radio- and Environmental Chemistry, 5232 Villigen PSI, Switzerland. E-mail: markus.ammann@psi.ch*
[b] *ETH Zurich, Institute for Atmospheric and Climate Science, 8092 Zurich, Switzerland*
[c] *Max Planck Institute for Chemistry, Multiphase Chemistry Department, 55128 Mainz, Germany*
† Current address: University of Cambridge, Department of Chemistry, Cambridge CB2 1EW, UK.

ozonolysis of protein films,[20] where a decrease in reactive uptake with decreasing humidity was ascribed to kinetic limitation by bulk diffusion. There are several other studies dealing with the influence of the physical state on reactivity; for instance, Kuwata and Martin showed that the formation of organonitrogen compounds in α-pinene SOA is contingent on high relative humidity (RH),[21] while Zhou *et al.* saw a clear limitation of the reaction of benzo[*a*]pyrene with ozone ($O_3$) under dry conditions when coated with α-pinene SOA.[22] In all three studies, changes in the physical state were induced by varying RH, as water can act as a plasticiser for water soluble compounds.

In this study, we for the first time provide a full map of such a heterogeneous reaction system – ozonolysis of shikimic acid – by probing a large range of humidity and $O_3$ concentration over long time scales in order to access the relevant kinetic regimes.

Shikimic acid ((3*R*,4*S*,5*R*)-3,4,5-trihydroxycyclohex-1-ene-1-carboxylic acid) is a carboxylic acid that has been detected in biomass burning aerosols.[23] It can be considered as a proxy for highly oxidised, water-soluble OM. Its cyclic double bond is expected to react with $O_3$ in a Criegee reaction,[24] cleaving the bond and leading to more highly oxidised reaction products. We have previously shown that shikimic acid undergoes humidity-induced glass transition[25] and that changes in humidity are accompanied by changing degradation rates, as assessed by scanning transmission X-ray microscopy (STXM), combined with near edge X-ray absorption fine structure (NEXAFS) spectroscopy.[26] On the long timescales observable in the STXM-NEXAFS experiments, this behaviour was found to be most consistent with classic reaction–diffusion limited kinetics with shikimic acid being well-mixed and $O_3$ showing a pronounced concentration gradient. However, due to low time resolution of these measurements and difficulties to quantify $O_3$ concentrations, further experiments are needed. In this study, we use coated wall flow tube (CWFT) measurements to investigate the changing kinetics of glass-forming organics under changing environmental conditions and employ a resistor model approach to evaluate the experimental data. The comprehensive data set presented here will also allow application of the more detailed kinetic multi-layer model[27] in follow up studies to constrain reaction and transport parameters not accessible *via* the resistor model approach.

# Methods

## Experimental

**Apparatus.** All uptake experiments were conducted using an atmospheric pressure CWFT reactor (length 48 cm, inner diameter 1.2 cm) coupled to a commercial $O_3$ analyser (Photometric $O_3$ Analyser – Model 400E; TELEDYNE Instruments). The reactor tube was encased in a cooling jacket connected to a thermostat to regulate temperature within the reactor. Temperature was set to 22.5 °C throughout all experiments. The reactor is fitted with an injector system to facilitate reactant exposure under equilibrated conditions. The injector consists of a stainless steel rod with an inner polytetrafluoroethylene (PTFE) tube and a PTFE outlet with two openings on opposite sides of the cap. A mixed gas flow of $N_2$, $O_2$, $H_2O$ and $O_3$ is passed through the injector. The position of the outlet can be changed by moving the injector inside the reactor. When the outlet is located at the downstream end of the flow tube, the film is not exposed to $O_3$. The movement of the injector towards the upstream end of the flow tube exposes the flow tube coating to the injector gas flow and therefore to the reactant $O_3$. A second gas flow feeds into the reactor at the upstream end. This sheath gas flow prevents back flow and keeps the film equilibrated to the selected RH when not exposed to the injector flow. The RH is adjusted by bubbling both gas flows through water reservoirs located in the same thermostat bath. This way, RH stays constant upon exposure to the injector gas flow.

**Oxidant generation and flow conditions.** $O_3$ was generated by passing the mixed $O_2/N_2$ flow through a quartz tube exposed to a UV-source of adjustable intensity. The total flow rate through the photolysis cell was set to 520 ml $min^{-1}$ with the $O_2$ fraction varying between 20 and 100 ml $min^{-1}$. The $N_2$ sheath gas flow was set to 500 ml $min^{-1}$ for all experiments, leading to a total flow rate of 1020 ml $min^{-1}$ through the CWFT, of which 750 ml $min^{-1}$ were drawn into the $O_3$ analyser, while the excess passed into the venting system. Using the given flow rates and fine tuning *via* lamp intensity, the $O_3$ concentration was varied from 90 to 1984 ppb. All flows within this section are given for STP conditions. The Reynolds number under the applied flow conditions is 134, indicating laminar flow.

**Sample preparation.** Flow tube coatings were prepared from a solution of 5.0 mg of shikimic acid (≥99%, Sigma-Aldrich) in 600 μl ethanol (reagent ACS, VWR). Prior to sample application, the glass tube was etched with ~5% hydrofluoric acid. After application and distribution of the solution on the flow tube, the film was pre-equilibrated with a 500 ml $min^{-1}$ flow of 85% RH $N_2$ for at least 30 min. The pre-equilibrated flow tube was then inserted into the reactor casing for equilibration to the RH and temperature set for the respective experiment for at least 1 h. The coated glass tubes were visually inspected before and after each experiment. Under some conditions, crystallisation occurred, which was apparent from the appearance of the film changing from bright clear (barely visible) to turbid or structured with cracks, accompanied by a decrease in $O_3$ uptake. In that case, the experiment was discarded. Crystallisation occurred especially at low RH and higher temperature, probably due to the increased mobility. This is the reason why no useful dataset on the temperature dependence could be obtained.

**Measurements.** Before each measurement, the $O_3$ baseline concentration was monitored with the injector placed at the downstream end of the flow tube and hence in the absence of chemical reaction. After this initialisation period, the injector was moved to the upstream end of the flow tube to expose the shikimic acid film to $O_3$. The subsequent change in $O_3$ concentration was monitored over at least 14 h, after which the injector was moved back upstream to measure the $O_3$ concentration without reaction once more and detect potential drifts in the $O_3$ baseline. Such drifts in concentration could arise from fluctuations in the UV light intensity. For most experiments, an additional measurement of the $O_3$ baseline was performed

 

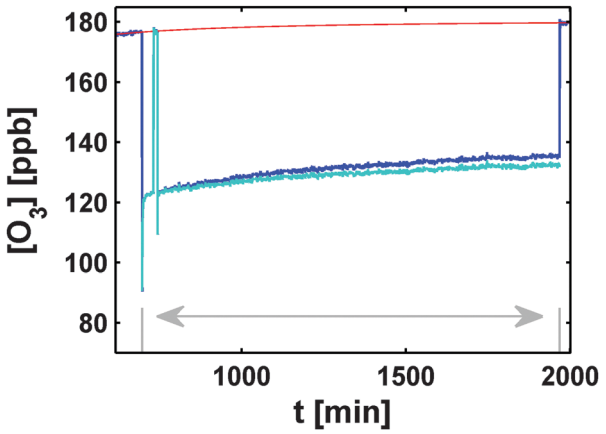


Fig. 1 Ozone mixing ratio downstream of the flow tube. Blue line: raw data of the $O_3$ loss as a function of time. Red line: power law fit to the $O_3$ baseline. Cyan line: corrected data (see text). Grey lines and arrow: time period of 21 h of exposure to $O_3$. Not shown: initialisation period (first 2 h).

after *ca.* 20 min of exposure to further constrain potential drifts. The $O_3$ baseline was interpolated using a power function: $f(x) = a + b{\cdot}x^c$. A minimum of three measurements at 177–179 ppb $O_3$ concentration were conducted at the following RH values: 0% RH, 24% RH, 45% RH, 69% RH, 83% RH and 92% RH. For two of these RH values, 24% and 92%, three measurements each were performed at three additional $O_3$ concentrations: 89–90 ppb, 495–496 ppb and 1984–1985 ppb. Fig. 1 shows the data of a measurement at 83% RH and 177 ppb $O_3$ before and after correction for drift in the $O_3$ baseline.

### Determination of the uptake coefficient

The uptake coefficient $\gamma$ describes the probability that a given gas molecule undergoing collision with a surface is subsequently taken up at that surface. It is defined as the net uptake normalised by the collision flux.[28] $\gamma$ can be extracted from the measured $O_3$ concentrations assuming that the decay over the length of the flow tube follows pseudo-first order kinetics at each sampling time. For well-mixed conditions in the gas phase, the decrease in $O_3$ can be described as:

$$\frac{d[O_3]_g}{dt} = -k^I[O_3]_g = -\gamma\frac{\omega_{O_3}}{4}\frac{S}{V_g}[O_3]_g \qquad (1)$$

where $[O_3]_g$ is the molecular number density of $O_3$ in the gas phase in $cm^{-3}$; $k^I$ [$s^{-1}$] is the pseudo-first order rate coefficient with respect to $O_3$; $\omega_{O_3}$ [cm $s^{-1}$] the mean thermal velocity of $O_3$ molecules; and $S/V_g$ [$cm^2$ $cm^{-3}$] the ratio of surface area to gas phase volume. The time coordinate is linked to the length coordinate along the tube, $l$, *via*: $t = \pi d^2 l/4\varphi$, where $d$ [cm] is the flow tube diameter and $\varphi$ [$cm^3$ $s^{-1}$] the volumetric flow rate. As $[O_3]_{g,0}$, the number density of $O_3$ at the entrance of the tube, is assumed to remain constant during the measurements, in principle, $\gamma$ can be determined from $[O_3]_{g,0}$ and the measured value at $[O_3]_{g,48\,cm}$ (corresponding to the downstream end of the flow tube at $l$ = 48 cm) at each sampling time during $O_3$ exposure. However, in reality, conditions in the flow tube are not perfectly well mixed, and corrections for the gradient arising from gas phase diffusion have to be made. We are using the diffusion correction by Murphy and Fahey,[29] based on the work by Cooney *et al.*[30] For this method, referred to as CKD (Cooney, Kim, Davis), the differential equation that governs the mixing ratio of the analyte as a function of axial and radial positions in a cylindrical geometry under axial flow is solved using the boundary condition that a constant fraction of wall collisions result in reaction. This yields a transmission ratio corrected for wall loss. The calculated transmission ratios are then fitted to the experimental transmission ratio to determine the corrected value for $\gamma$. Both eqn (1) and the CKD method assume a first-order uptake process. However, in general, this is not granted *a priori*, and as also shown in this study, $\gamma$ may depend on the gas phase concentration, more specifically, on its inverse in the saturating regime of a Langmuir–Hinshelwood type surface reaction limited uptake process.[31] Thus, in this extreme case, the uptake becomes zero-order, which leads to a linear decrease of the reactant concentration with time rather than an exponential as for first-order decay under well-mixed conditions. For small losses of the gas phase ozone concentration, the effect on the resulting value of $\gamma$ is negligible. For the range of $\gamma$ in this study, where the uptake deviates indeed from first order behaviour, $3 \times 10^{-6} - 7 \times 10^{-7}$, $\gamma$ is overestimated by at maximum 11–4%, respectively. Since the uptake also changes rapidly with time in the relevant period, no attempt has been made to further correct the data for this.

## Results and discussion

The progression of $O_3$ uptake with exposure time was measured at different RH and $O_3$ concentrations. Fig. 2 shows $\gamma$ as a function of time at six different RH and a fixed $O_3$ concentration of 177–179 ppb. The general progression is similar for all measurements: initially a plateau develops, which after about 2 min decreases to a lower, relatively stable long-term

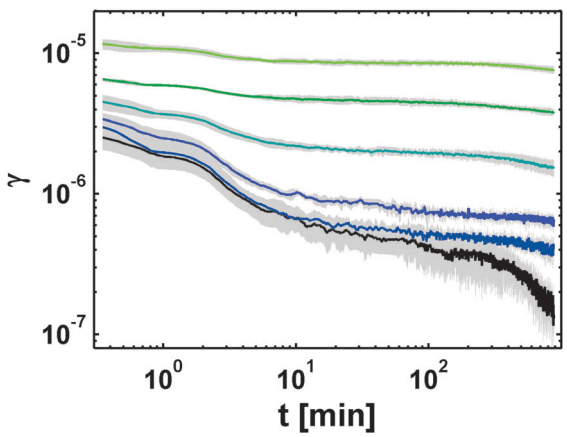


Fig. 2 Evolution of $\gamma$ at 177–179 ppb $O_3$ at six different humidities. From the bottom up: 0% RH (black), 24% RH (dark blue), 45% RH (blue), 69% RH (dark cyan), 83% RH (green) and 92% RH (bright green). Areas shaded in grey denote the standard deviations of the averaged measurements.

uptake, which after about 1 h slowly declines further, especially at lower humidity. With decreasing RH, $\gamma$ decreases by about one order of magnitude from $8.7 \times 10^{-6}$ at 92% RH to $6.0 \times 10^{-7}$ at 0% RH (averaged value at 11 to 16 min exposure). The relative magnitude of the decrease from the initial plateau to the long-term value becomes smaller at higher RH, and the slope of the decrease in long-term uptake increases with decreasing RH. As the slope of the decrease depends on whether and how the baseline drift is corrected, there is some uncertainty in the exact slope. This is true in particular for uptake at low RH, where the absolute $O_3$ loss is small. However, the general trend in $\gamma$ between measurements at different RH is clear and consistent with and without correction of the baseline drift.

The dependence of $\gamma$ on the $O_3$ concentration at 24% RH and 92% RH is shown in Fig. 3. In both cases, the height of the initial plateau decreases with increasing $O_3$ concentration until it basically vanishes at 1984–1985 ppb. The decrease of the initial plateau with increasing $O_3$ points toward saturation of adsorption sites at the particle surface at high $[O_3]_g$, which is consistent with a Langmuir–Hinshelwood type reaction present in this time regime.[31] At long reaction times, at 24% RH, the steady-state uptake ($\geq 10^1$ min) decreases almost constantly while at 92% RH, an accelerating reduction in $\gamma$ at the highest $O_3$ concentrations points toward a complete depletion of the organic film at the end of the measurements ($\geq 10^3$ min). Integration of the measured $O_3$ loss over time yields a total loss of $1.66 \times 10^{19}$ $O_3$ molecules. This is very close to the total number of shikimic acid molecules in the film ($1.72 \times 10^{19}$), which confirms that the steeper decrease at these high $O_3$ concentrations at simultaneously high RH is caused by depletion of shikimic acid in the whole CWFT film. We note that the primary reactive loss channel in this system is expected to be the reaction with shikimic acid. The reaction with water (*via* $O_3 + OH^-$, $k^{II} = 70\ M^{-1}\ s^{-1}$ [32]) is negligible under our conditions.

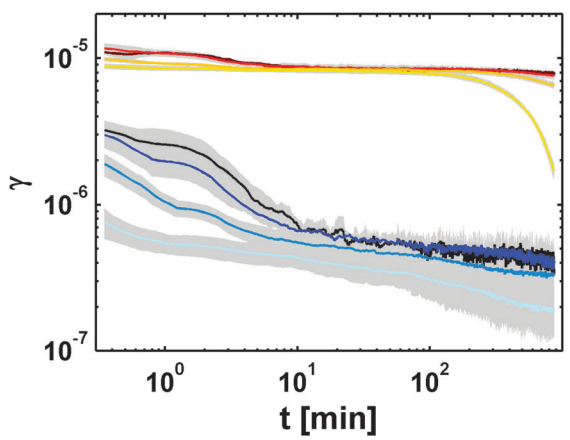


Fig. 3 Evolution of $\gamma$ at four different concentrations of $O_3$ at two different humidities: 24% RH (89–90 ppb (black), 177–179 ppb (blue), 495–496 ppb (dark cyan), 1984–1985 ppb (light blue)) and 92% RH (89–90 ppb (dark red), 177–179 ppb (red), 495–496 ppb (orange), 1984–1985 ppb (yellow)). Areas shaded in grey denote the standard deviations of the averaged measurements.

The uptake coefficient of $O_3$ to pure water could not be measured in our CWFT. We refer to a recent study[33] of our group, where the upper limit for the uptake coefficient has been reported as $10^{-7}$.

### Steady-state evaluation

As concluded from the shapes of the uptake curves above, at least two different reactive loss processes, surface and bulk reactions, must be involved in the total $O_3$ loss. In the case of multiple loss processes, a resistor model can be applied to describe the system under steady-state assumptions. We note that while the system is not in the steady state over the full duration of the experiments, $\gamma$ varies only to a small degree over shorter time periods. These short time periods are still orders of magnitude longer than the residence time of reactive gas in the flow tube, so that 'quasi-steady state' can be assumed. The resistor model formulation for species X undergoing both surface and bulk reactions is accordingly:[34]

$$\frac{1}{\gamma} = \frac{1}{\alpha_{s,0}} + \frac{1}{\dfrac{1}{\dfrac{1}{\Gamma_b} + \dfrac{k_d}{\alpha_{s,0} k_{sb}}} + \Gamma_s} \qquad (2)$$

where $\alpha_{s,0}$ is the surface accommodation coefficient on a free substrate, $1/\Gamma_s$ the resistance for uptake *via* surface reaction and $1/\Gamma_b$ the resistance for uptake *via* bulk reaction. $k_d$ is the desorption rate coefficient. Its inverse corresponds to desorption lifetime $\tau_d$. $k_{sb}$ is the solvation rate coefficient, describing the transformation from a surface molecule (adsorbed) to a bulk phase (dissolved) molecule for volatile species.

**Surface reaction-dominated regime.** Given the recommended bulk accommodation coefficient for $O_3$ on water ($>10^{-3}$)[34] and assuming that surface accommodation is not limiting bulk accommodation, it is unlikely that surface accommodation is the rate limiting step. Eqn (2) then simplifies to

$$\gamma = \frac{1}{\dfrac{1}{\Gamma_b} + \dfrac{k_d}{\alpha_{s,0} k_{sb}}} + \Gamma_s \qquad (3)$$

where $\Gamma$ is the sum of a bulk process (solvation and bulk reaction) and a surface reaction. The surface reaction can therefore be separated as $\Gamma_s$ contributes additively to $\gamma$. We assume that the decrease of the initial plateau indicates the end of surface reaction, and therefore chose $\gamma$ averaged at 11–15 min to represent the uptake probability associated with the initial bulk process, $\Gamma_b$. The surface part, $\Gamma_s$, can then be extracted by subtracting $\Gamma_b$ from the total $\gamma$ measured on the initial plateau. The results are shown in Fig. 4. The substantial uncertainty associated with this treatment amounts to at least a factor of 3 in both directions for $\Gamma_s$ (error bars not shown). The values determined for $\Gamma_s$ at 24% RH are only within a factor of 1.2 and 2.3 lower than for 92% RH, which is a relatively small difference compared to the difference in the overall $\gamma$ of more than one order of magnitude measured on the second, bulk dominated plateau. This suggests that the surface reaction is not strongly influenced by changes in humidity. The uptake coefficient of a

 

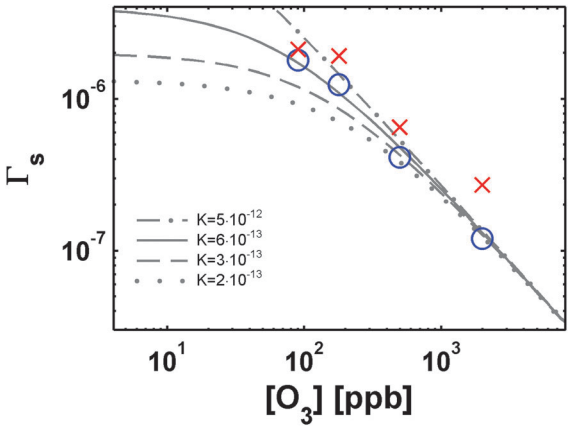


Fig. 4 Dependence of $\Gamma_s$ on $O_3$ concentration. Blue circles show experimental data at 24% RH, red crosses at 92% RH. The grey lines show fits of eqn (4) to the experimental data at 24% RH, using the following values: $k^I_{SLR} = 2 \times 10^{-4}$ s$^{-1}$, $N_{max} = 3 \times 10^{14}$ cm$^{-2}$ and $K_{ads,O_3} = 5 \times 10^{-12}$ cm$^3$ molecule$^{-1}$ (dash-dotted line), $6 \times 10^{-13}$ cm$^3$ molecule$^{-1}$ (solid line), $3 \times 10^{-13}$ cm$^3$ molecule$^{-1}$ (dashed line), and $2 \times 10^{-13}$ cm$^3$ molecule$^{-1}$ (dotted line).

Langmuir–Hinshelwood surface reaction of $O_3$ with a second species Y residing on the surface can be described by the following equations:[31]

$$\Gamma_s = \frac{4k^I_{SLR} K_{ads,O_3}}{\omega_{O_3}\sigma_{O_3}\left(1 + K_{ads,O_3}[O_3]_{gs}\right)} \quad (4)$$

with

$$K_{ads,O_3} = \frac{\omega_{O_3}\sigma_{O_3}\alpha_{s,0}}{4k_d} \quad (5)$$

and

$$k^I_{SLR} = k^{II}_{SLR}[Y]_s \quad (6)$$

where $k^I_{SLR}$ is the first-order surface layer reaction rate coefficient in s$^{-1}$, $\sigma_{O_3}$ the occupied surface area per adsorbed molecule of $O_3$ in cm$^2$ molecule$^{-1}$, $K_{ads,O_3}$ the Langmuir constant in cm$^3$ molecule$^{-1}$, describing the adsorption–desorption equilibrium, $k^{II}_{SLR}$ the second order surface layer reaction rate coefficient in cm$^2$ s$^{-1}$ and $[Y]_s$ the surface concentration of Y, in units of molecule cm$^{-2}$ s$^{-1}$. Eqn (4) reveals that the decrease in $\Gamma_s$ with increasing $[O_3]_{gs}$ at high concentrations is caused by the limited availability of adsorption sites, because then, $K_{ads,O_3}[O_3]_{gs} \gg 1$, so that the denominator in Eqn (4) increases linearly with $[O_3]_{gs}$ leading to the decrease of $\Gamma_s$.[31] Eqn (4) was fitted to the experimental data. In the form written above, we have three unknown variables in the equation: $K_{ads,O_3}$, $k^I_{SLR}$, and $\sigma_{O_3}$. $1/\sigma_{O_3}$ equals $N_{max}$, the number of adsorbed molecules of $O_3$ on a fully-covered surface per cm$^2$. In the high concentration limit, the slope of a double logarithmic plot of $\gamma$ against $[O_3]_g$ is $-1$ (*cf.* Fig. 4), indicating the inverse relationship of eqn (4). While changing $k^I_{SLR}$ and $N_{max}$ causes a vertical parallel shift of the fitting curve in Fig. 4, the position of the inflection point of the fitting curve (transition to the low concentration regime) depends on $K_{ads,O_3}$. It is therefore only possible to determine $3 \times 10^{-13}$ cm$^3$ molecule$^{-1}$ as a lower limit for $K_{ads,O_3}$ (dashed curve in Fig. 4). At lower $K_{ads,O_3}$ values, the absolute values of the plateau could still be adjusted *via* $k^I_{SLR}$ and $N_{max}$, but the transition into the regime with inverse dependence of gamma with $[O_3]_g$ would occur at too high $O_3$ concentration. However, the available data do not allow the determination of an upper limit for $K_{ads,O_3}$. While the data points do indicate a slight curvature that could be interpreted as the beginning of the low concentration plateau, the error is too large to draw this conclusion. Measurements at lower $[O_3]_g$ would be needed to determine at which concentration the slope decreases. The uncertainty around the transition into zero-order uptake in this regime of uptake and the corresponding small overestimation of $\gamma$ and thus $\Gamma_s$ does not change the assessment of the lower limit. The lower limit of $K_{ads,O_3} = 3 \times 10^{-13}$ cm$^3$ molecule$^{-1}$ compares well with $K_{ads,O_3}$ values for ozonolysis of polycyclic aromatic hydrocarbons (PAHs) such as benzo[*a*]pyrene, where $K_{ads,O_3}$ is between $1.2 \times 10^{-15}$ cm$^3$ molecule$^{-1}$ [35] and $2.8 \times 10^{-13}$ cm$^3$ molecule$^{-1}$ [36] and anthracene, where $K_{ads,O_3}$ ranges from $2.2 \times 10^{-15}$ cm$^3$ molecule$^{-1}$ to $1.0 \times 10^{-13}$ cm$^3$ molecule$^{-1}$.[37] While it is not possible to separate $k^I_{SLR}$ and $N_{max}$ from the data, $7 \times 10^{14}$ cm$^{-2}$ could be taken as an upper limit for $N_{max}$.[34,38] This gives a value of around $7 \times 10^{-5}$ s$^{-1}$ as the lower limit for $k^I_{SLR}$.

We also estimated the $O_3$ loss due to the surface reaction by subtracting the integral of the $O_3$ loss due to bulk processes from the integral of the total loss for the time period of up to 8 min. The integrated $O_3$ loss from bulk processes was estimated in two different ways. In the first case, the average ozone loss at 11–15 min was used to calculate the bulk integral (linear, horizontal extrapolation). In the second case, a power function ($f(x) = a \cdot x^b$) fitted to the $O_3$ loss between 10 and 100 min was used to extrapolate the $O_3$ loss due to bulk processes for up to 8 min. The integrated surface $O_3$ loss from the two methods is within 1 ($\pm$0.5) $\times 10^{15}$ molecules, which is only slightly more than a monolayer. The differences between results obtained from both methods are not significant. Thus these first plateaus are caused by surface reaction, although a relatively small difference in the value obtained for the integral surface loss between low and high RH is somewhat surprising and could indicate that shikimic acid is a slight surfactant exhibiting similar surface coverages at high (the more dilute solution) and low RH. This may then also be the reason why the slope of the fall-off of $\Gamma_s$, and thus the adsorption properties, are similar for low and high RH. Hence, in the first five minutes, reaction is likely to proceed mainly in the Langmuir–Hinshelwood-dominated surface reaction regime. This surface reaction is saturated with respect to adsorption sites, even at the lowest investigated ozone concentrations of 79 ppb.

**Reaction–diffusion-limited regime.** After the decrease of the first plateau during the first minutes of the exposure, the system settles into a slowly declining pseudo steady-state uptake, which, as described above, may be bulk reaction dominated. In this case eqn (2) simplifies to

$$\frac{1}{\gamma_X} = \frac{k_d}{\alpha_{s,0}k_{sb}} + \frac{1}{\Gamma_b} = \frac{1}{\alpha_{b,0}} + \frac{1}{\Gamma_b} \quad (7)$$

Considering the IUPAC-recommended value of $\alpha_{b,0} > 1 \times 10^{-3}$ for $O_3$ on water,[34] the contribution of $\alpha_{b,0}$ to the total resistance is negligible and the equation simplifies to

$$\gamma_X = \Gamma_b \quad (8)$$

Given that the condensed phase is liquid at 92% RH, and that the time scale to react away all shikimic acid takes over 15 hours at the highest $O_3$ concentration (Fig. 3), the reaction rate must be slow, so that both $O_3$ and shikimic acid should be well-mixed within a large part of the bulk. We can then assume a bulk reaction-limited case to determine the second-order rate coefficient of the reaction from the following equation:[34]

$$k_{BR}^{II} = \frac{\gamma_X \omega_{O_3} \frac{S}{V_b}}{4HRT[Y]_b} \quad (9)$$

where $k_{BR}^{II}$ is the second-order rate coefficient of the bulk reaction, $S/V_b$ the ratio of film surface to film volume, $H$ the Henry's law constant, $R$ the gas constant, $T$ the temperature and $[Y]_b$ the concentration of shikimic acid in the film. We are using $H = 1.2 \times 10^{-2}$ mol L$^{-1}$ atm$^{-1}$ for $O_3$ in water[39] and shikimic acid at a concentration of 3.38 mol L$^{-1}$. The shikimic acid bulk concentrations and film thicknesses were deduced from hygroscopicity measurements of levitated particles in an electrodynamic balance (EDB).[25] The calculated second-order rate coefficient is $1.7 \times 10^3$ L mol$^{-1}$ s$^{-1}$. Note that using concentration in mol L$^{-1}$ instead of activity as a metric induces uncertainty in the reported rate coefficient. As will be discussed further below, also Henry's law constants for these solutions are not well established. Since the true observable of the experiment would be the product $k_{BR}^{II} H [Y]_b a_Y$, with $a_Y$ denoting the activity coefficient of Y, we remain with molarity to characterise the solution concentration in the absence of reliable activity coefficients.

The reacto-diffusive length, $l_{O_3}$, describes the characteristic length a gas-phase molecule can diffuse into the bulk before it reacts. At a distance $l_{O_3}$ from the surface, the $O_3$ concentration in the bulk dropped to 1/e of its initial value. $l_{O_3}$ can be calculated by the following equation:[40]

$$l_{O_3} = \sqrt{\frac{D_{b,O_3}}{k_{BR}^{II}[Y]_b}} \quad (10)$$

where $D_{b,O_3}$ is the diffusion coefficient of $O_3$ in the bulk. It can be estimated by applying the Stokes–Einstein equation, $D_{b,O_3} = k_B T/(6\pi\eta r_{O_3})$, where $k_B$ is the Boltzmann constant, $\eta$ the dynamic viscosity and $r_{O_3}$ the molecular radius of $O_3$. Using the diffusion coefficient of water, $D_{H_2O}$, in shikimic acid at 92% RH,[25] we can estimate the diffusion coefficient of $O_3$ by $D_{b,O_3} = D_{H_2O} r_{H_2O}/r_{O_3}$. Using $1.1 \times 10^{-6}$ cm$^2$ s$^{-1}$ at 92% RH we obtain $l_{O_3} = 252$ nm. As this is only about half of the total film thickness of 471 nm at 92%, $O_3$ is clearly not well-mixed over the complete volume of the bulk as assumed above. To adjust for the decrease of $[O_3]$ with increasing film thickness $d$, we replace the bulk volume $V_b$ with an effective volume, where the film thickness has been replaced by an effective depth $d_e$ over which volume limited $O_3$ loss occurs. Assuming an exponential decrease of $[O_3]$ with increasing film depth, $d_e$ can be calculated as

$$d_e = \int_0^d e^{-\frac{x}{l_{O_3}}} dx \quad (11)$$

where $x$ is the penetration depth. This correction leads to a second-order rate coefficient of 3.7 $(+1.5/-3.2) \times 10^3$ L mol$^{-1}$ s$^{-1}$. The stated error contains the uncertainties of measured variables as well as an estimation of the maximum error caused by uncertainties in Henry's law constant. The solubility of $O_3$ tends to increase slightly with decreasing polarity of the solvent.[41] If the solubility changes due to the presence of shikimic acid, $H$ should therefore increase ("salting in"). We chose the Henry constant of $O_3$ in acetic acid[41] to calculate the upper bound for this effect. To estimate a lower limit of the Henry constant, we chose the lowest value for $H$ [mol L$^{-1}$ atm$^{-1}$] from a compilation of Henry's law constants of $O_3$ in water,[42] excluding values without primary literature references. Within its uncertainty, the value for the rate coefficient is the same as for the second order rate constant determined from STXM-NEXAFS measurements ($3 \times 10^3$ L mol$^{-1}$ s$^{-1}$), which was derived from the degradation rate of shikimic acid.[26] The rate constant is therefore showing good agreement between the two techniques. It should be noted that the measurement used for the extraction of the rate constant using STXM was conducted at a lower humidity (82% RH) and assuming only reaction limitation; its value for $k_{BR}^{II}$ is therefore likely underestimated. The rate coefficient of shikimic acid with $O_3$ determined here is comparable to similarly functionalised compounds in aqueous solution, such as maleic acid ($1 \times 10^3$ L mol$^{-1}$ s$^{-1}$) and fumaric acid ($6 \times 10^3$ L mol$^{-1}$ s$^{-1}$).[43] It is about three orders of magnitude lower than the second-order rate coefficient of $O_3$ and oleic acid ($1 \times 10^6$ L mol$^{-1}$ s$^{-1}$),[44] a compound frequently used as a proxy for the assessment of condensed phase oxidation kinetics of OM.[45]

The previous considerations are all based on the 92% data set, where the assumption of volume limited uptake allowed us to obtain a reasonable estimate of the second order rate coefficient directly from the uptake coefficient. With decreasing humidity, the uptake decreases despite the increase in shikimic acid concentration. Since the condensed phase becomes more and more viscous, diffusion of $O_3$ into the bulk becomes slower. Reacto-diffusive limitation of the uptake could in principle explain the decrease in $\gamma_X$ with decreasing humidity. In the following, we will investigate this hypothesis. Reacto-diffusive uptake is described by the following equation:[34]

$$\Gamma_b = \frac{4HRT}{\omega_{O_3}} \sqrt{D_{b,O_3} k_{BR}^{II} [Y]_b} \quad (12)$$

Fig. 5b shows the values of the averaged uptake coefficient at time 11–15 min as a function of relative humidity. The general trend of decreasing steady-state ozone uptake with decreasing RH is consistent with our previous STXM study. The solubility of ozone, in general, increases rather slightly with decreasing polarity of organic solvents and will be assumed constant. If we also assume that the reaction rate coefficient is independent of

 

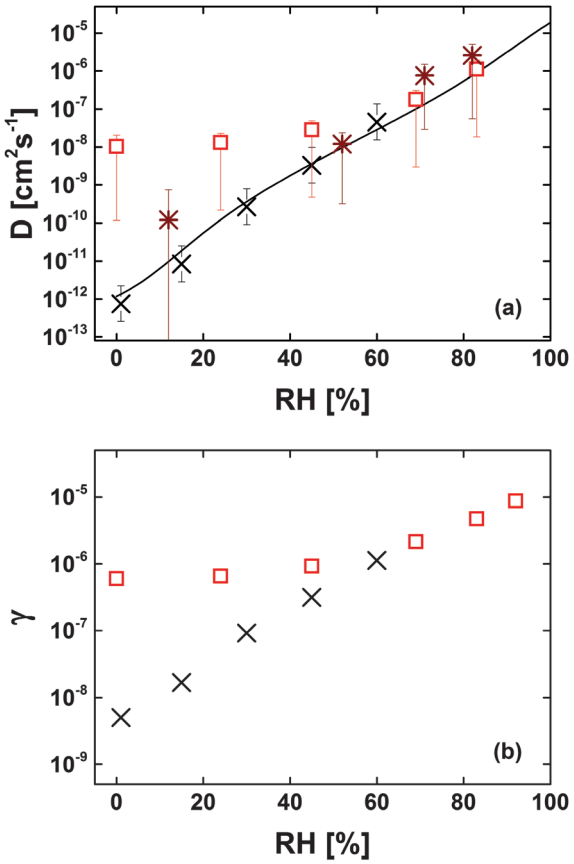


Fig. 5 (a) $O_3$ diffusion coefficients from flow tube (295.7 K, red squares) and STXM (~298 K, dark red asterisks) measurements as well as water diffusion coefficients from EDB measurements (293.5 K, measured data: black crosses, parameterisation: black line). (b) Humidity dependent $O_3$ uptake measured in this study (red squares) and calculated from $D_{b,H_2O}$ (parameterised from EDB data and assuming reacto-diffusive limitation, black crosses).

the shikimic acid concentration, the obvious parameter varying with water content is the diffusion coefficient. The squares in Fig. 5a hence represent the $D_{b,O_3}$ necessary to obtain the measured uptake coefficients according to eqn (12), with all other parameters kept constant except the shikimic acid concentration. The diffusion coefficients for this flow tube study are compared with $D_{b,O_3}$ data inferred from the STXM-NEXAFS experiments[26] as well as $D_{b,H_2O}$ determined from EDB measurements.[25] The values for all three techniques agree well at higher RH. While the diffusion coefficients determined for water *via* EDB and those for $O_3$ inferred from the STXM-NEXAFS measurements are also in agreement at low RH; values derived from $\Gamma_b$ in this study are consistently larger below 45% RH. At 0% RH, the value for $D_{b,O_3}$ determined from the flow tube measurements is four orders of magnitude larger than the one derived from the EDB measurements. In turn, uptake coefficients calculated from eqn (10) through insertion of the $D_{b,H_2O}$ measured with the EDB are much smaller than $\gamma$ actually measured in the flow tube (Fig. 5b). While the diffusion coefficient measured *via* EDB was for water and not $O_3$, the molecules are sufficiently similar that the difference in molecular size is unlikely to explain the large difference observed between measured diffusion coefficients and those inferred from $\Gamma_b$. It is therefore clear that eqn (12) does not adequately describe the reaction system at low RH.

At 69% RH, using $D_{b,O_3} = 1.8 \times 10^{-7}$ cm$^2$ s$^{-1}$, $l_{O_3}$ is 28 nm. Given the film thickness of 250 nm, this clearly indicates reaction–diffusion limitation. As the discrepancy between $D_{b,H_2O}$ and the effective $D_{b,O_3}$ determined above indicates that the shikimic acid–$O_3$–water system does not follow pure reaction–diffusion limitation at and below 45% RH, we refrain from determining $l_{O_3}$ at RH $\leq$ 45%. $l_{O_3}$ was determined to be about 1 nm at 12% RH in our previous STXM/NEXAFS study.[26] Deviations from the reaction–diffusion regime were expected at very low RH due to the decreasing diffusivity of shikimic acid, which the resistor model cannot account for. The characteristic chemical lifetime of shikimic acid is

$$\tau_Y = \frac{1}{k_{BR}^{II}[O_3]_b} \quad (13)$$

At 500 ppb, $\tau_Y$ is about $5 \times 10^4$ s. The upper limit of $D_{b,Y}$ for mass transport limitation of the reaction due to diffusion of shikimic acid would be given when diffusion becomes too slow to transport shikimic acid from the bottom of the film to the surface within $\tau_Y$. The upper limit for $D_{b,Y}$ can therefore be calculated with

$$D_{b,Y} = \frac{d^2}{2\tau_Y} \quad (14)$$

Using the film thickness at 0% RH (185 nm), $D_{b,Y} \approx 4 \times 10^{-15}$ cm$^2$ s$^{-1}$ is the upper limit for diffusion limitation with regards to shikimic acid. Such low diffusivities can occur for self-diffusion of organic molecules when the material is solid or highly viscous semi-solid.[9,12,20] However, in that case the uptake should be lower than expected, not higher, as observed in this study.

A possible explanation for the unexpectedly high uptake at low RH is the occurrence of an $O_3$ self-reaction, likely involving long-lived reactive oxygen intermediates or other first generation intermediates or products.[46] Such a self-reaction has been suggested to govern the long-term $O_3$ uptake to soot.[47] In the absence of surface sensitive analysis tools, the nature of the species involved in detail remains speculative. At low RH, when the overall uptake is low, such a reaction could significantly contribute to the total $O_3$ loss to shikimic acid in our case. Assigning the total uptake to a bulk reaction only leads to an overestimation of $D_{b,O_3}$ and, to a lesser extent, $k_{BR}^{II}$ as determined from high RH experiments. In a scenario with uptake being strongly influenced by self-reaction on the surface, a limitation due to mass transport of shikimic acid would also go undetected. We note that in the STXM experiment, $D_{b,O_3}$ was derived from the degradation rate of shikimic acid, and not from the uptake of $O_3$, so that it was not affected by a potentially active self-reaction of $O_3$ on the surface. Inclusion of the self-reaction as a resistance term is not possible within the resistor formulation used for the data analysis in this study. We also note that other parameters, such as the activity coefficients

and Henry's law constant remain uncertain at low RH, which makes a quantitative attribution of a surface reaction component a difficult task. A more detailed explicit kinetic model[27] is needed to address this point further.

### Limitations of the traditional resistor-model approach

As explained in the previous section, the resistor model can be used to interpret the initial plateau as well as the RH dependence of the long-term uptake at higher RH (>60%). However, its application to data at lower humidity leads to results which are only consistent with measurements with other techniques if we invoke a significant contribution of an $O_3$ self-reaction on the surface to the $O_3$ uptake.

We assume that the initial plateau in the reactive uptake data is due to a surface reaction, which decreases after the first couple of minutes due to consumption of shikimic acid initially present on the surface. This depletion of shikimic acid at the surface points towards mass transfer limitation from the bulk to the surface, as the concentration would otherwise be constantly replenished. At low RH, such a limitation in mass transfer could be due to slow self-diffusion of shikimic acid to the near-surface region. However, this cannot explain the presence of the initial plateau at high RH as diffusion should be sufficiently fast to ensure immediate exchange. A possible explanation would be a particularly slow bulk–surface transfer (''desolvation'') of shikimic acid, which could be caused by the formation of a dense product layer at the surface within short time scales, shielding shikimic acid from reaction *via* the surface reaction pathway. For the dry conditions discussed above, the estimate of $l_{O_3}$ in the lowermost nm range and the lack of mixing due to the very low diffusivity of shikimic acid and products under dry conditions, would keep such a product layer extremely thin. This is also the reason, why a product layer could not be observed in our previous STXM/NEXAFS study, neither under dry nor wet conditions.[26] Apart from testing such a scenario with a more explicit model, more explicitly surface sensitive (at the molecular level) methods should be employed to address these.

Three additional features of the dataset cannot be explained by the traditional resistor model approach. The first is the slow decrease of the long-term uptake, which is particularly prominent for the dry experiment. The second is the dependence of the long-term uptake on the gas phase $[O_3]_g$. According to eqn (12), $\Gamma_b$ should be independent of the gas phase ozone concentration. This can be seen for the measurements at high relative humidity, but is not observed for the measurement at 24% RH (*cf.* Fig. 3). The third is the decrease of both the initial plateau and the long-term uptake over time at low RH. Steady-state assumptions are invalid when the uptake changes over time. An analytical expression for the solubility limited uptake and its change with time exist and can be used in the resistor-model. In this case, $\gamma$ is proportional to $t^{-0.5}$, where $t$ is time.[34] A double logarithmic plot of $\gamma$ *vs.* $t$ should then exhibit a slope of $-0.5$, which cannot be observed in the experimental data presented here. We thus assume that the region between the initial and the second plateau (3 min to 10 min) and the slow decline of the second plateau (>100 min) mark transition regimes, which cannot be interpreted with the resistor model. To avoid the limitations of the resistor model and to obtain a more complete understanding of the reaction kinetics, a more explicit kinetic model needs to be applied, which will be the topic of a follow up study.

## Conclusions

The ozonolysis of shikimic acid was measured for several $O_3$ concentrations (89–1985 ppb) and humidities (0–92%) for over 14 h. The data were analysed under steady-state assumptions using a resistor model. The results suggest a Langmuir–Hinshelwood-type surface reaction running parallel to a bulk reaction for the first few minutes of the experiment, after which the bulk reaction dominates. Uptake due to surface reaction remains similar going from the aqueous solution at 92% RH to the semi-solid or solid material at 24% RH. The lower limit for $k_{SLR}^{I}$ was determined to be $4 \times 10^{-5}$ s$^{-1}$. The lower limit for $K_{ads,O_3}$ is $3 \times 10^{-13}$ cm$^3$, which compares well with $K_{ads,O_3}$ values for ozonolysis of PAHs. The uptake is best described by reaction limitation at 92% RH and reaction–diffusion limitation below 92% RH. The second order rate coefficient in the bulk was determined from the measurements at 92% RH. Its value of $3.7\ (+1.5/-3.2) \times 10^3$ L mol$^{-1}$ s$^{-1}$ is consistent with the one determined from STXM experiments.[26] The uptake increased by more than an order of magnitude upon humidification from 0 to 92% RH. This trend of increasing uptake with increasing humidity is again consistent with the finding from the STXM measurements. The steady state analysis reveals deficiencies in explaining the humidity dependent $\gamma$ after long exposure times when attributed to a reacto-diffusive regime. Additionally, the diffusion constants for $O_3$ are too high at low humidity, providing further evidence that the analytical expression for reacto-diffusive limitation does not adequately describe the system.

## Acknowledgements

We acknowledge support by the Swiss National Science Foundation (grant no. 130175) and the EU FP7 project PEGASOS. T. B. was supported by the Max Planck Graduate Center with the Johannes Gutenberg-Universität Mainz (MPGC). We thank M. Birrer for technical support and C. Marcolli for helpful discussions. F. Vivian ran preliminary experiments on the temperature dependence of the $O_3$ uptake. A. J. Huisman suggested shikimic acid as a possible proxy for glass-forming organic matter.

## Notes and references

1 M. Kanakidou, J. H. Seinfeld, S. N. Pandis, I. Barnes, F. J. Dentener, M. C. Facchini, R. van Dingenen, B. Ervens, A. Nenes, C. J. Nielsen, E. Swietlicki, J. P. Putaud, Y. Balkanski, S. Fuzzi, J. Horth, G. K. Moortgat, R. Winterhalter, C. E. L. Myhre, K. Tsigaridis, E. Vignati,

E. G. Stephanou and J. Wilson, *Atmos. Chem. Phys.*, 2005, **5**, 1053–1123.
2 Q. Zhang, J. L. Jimenez, M. R. Canagaratna, J. D. Allan, H. Coe, I. Ulbrich, M. R. Alfarra, A. Takami, A. M. Middlebrook, Y. L. Sun, K. Dzepina, E. Dunlea, K. Docherty, P. F. DeCarlo, D. Salcedo, T. Onasch, J. T. Jayne, T. Miyoshi, A. Shimono, S. Hatakeyama, N. Takegawa, Y. Kondo, J. Schneider, F. Drewnick, S. Borrmann, S. Weimer, K. Demerjian, P. Williams, K. Bower, R. Bahreini, L. Cottrell, R. J. Griffin, J. Rautiainen, J. Y. Sun, Y. M. Zhang and D. R. Worsnop, *Geophys. Res. Lett.*, 2007, **34**, L13801.
3 D. L. Bones, D. K. Henricksen, S. A. Mang, M. Gonsior, A. P. Bateman, T. B. Nguyen, W. J. Cooper and S. A. Nizkorodov, *J. Geophys. Res.*, 2010, **115**, D05203, DOI: 10.1029/2009JD012864.
4 O. Vesna, S. Sjogren, E. Weingartner, V. Samburova, M. Kalberer, H. W. Gäggeler and M. Ammann, *Atmos. Chem. Phys.*, 2008, **8**, 4683–4690.
5 M. Segal-Rosenheimer and Y. Dubowski, *J. Phys. Chem. C*, 2007, **111**, 11682–11691.
6 U. Pöschl and M. Shiraiwa, *Chem. Rev.*, 2015, **115**, 4440–4475.
7 J. F. Pankow, *Atmos. Environ.*, 1994, **28**, 189–193.
8 J. R. Odum, T. Hoffmann, F. Bowman, D. Collins, R. C. Flagan and J. H. Seinfeld, *Environ. Sci. Technol.*, 1996, **30**, 2580–2585.
9 T. Koop, J. Bookhold, M. Shiraiwa and U. Poschl, *Phys. Chem. Chem. Phys.*, 2011, **13**, 19238–19255.
10 A. Virtanen, J. Joutsensaari, T. Koop, J. Kannosto, P. Yli-Pirila, J. Leskinen, J. M. Makela, J. K. Holopainen, U. Pöschl, M. Kulmala, D. R. Worsnop and A. Laaksonen, *Nature*, 2010, **467**, 824–827.
11 T. D. Vaden, D. Imre, J. Beranek, M. Shrivastava and A. Zelenyuk, *Proc. Natl. Acad. Sci. U. S. A.*, 2011, **108**, 2190–2195.
12 E. Abramson, D. Imre, J. Beranek, J. Wilson and A. Zelenyuk, *Phys. Chem. Chem. Phys.*, 2013, **15**, 2983–2991.
13 C. L. Loza, M. M. Coggon, T. B. Nguyen, A. Zuend, R. C. Flagan and J. H. Seinfeld, *Environ. Sci. Technol.*, 2013, **47**, 6173–6180.
14 C. D. Cappa and K. R. Wilson, *Atmos. Chem. Phys.*, 2011, **11**, 1895–1911.
15 L. Renbaum-Wolff, J. W. Grayson, A. P. Bateman, M. Kuwata, M. Sellier, B. J. Murray, J. E. Shilling, S. T. Martin and A. K. Bertram, *Proc. Natl. Acad. Sci. U. S. A.*, 2013, **110**, 8014–8019.
16 H. C. Price, J. Mattsson, Y. Zhang, A. K. Bertram, J. F. Davies, J. W. Grayson, S. T. Martin, D. O'Sullivan, J. P. Reid, A. M. J. Rickards and B. J. Murray, *Chem. Sci.*, 2015, **6**, 4876–4883.
17 M. Shiraiwa, A. Zuend, A. K. Bertram and J. H. Seinfeld, *Phys. Chem. Chem. Phys.*, 2013, **15**, 11441–11453.
18 V. Perraud, E. A. Bruns, M. J. Ezell, S. N. Johnson, Y. Yu, M. L. Alexander, A. Zelenyuk, D. Imre, W. L. Chang, D. Dabdub, J. F. Pankow and B. J. Finlayson-Pitts, *Proc. Natl. Acad. Sci. U. S. A.*, 2012, **109**, 2836–2841.
19 T. Berkemeier, A. J. Huisman, M. Ammann, M. Shiraiwa, T. Koop and U. Pöschl, *Atmos. Chem. Phys.*, 2013, **13**, 6663–6686.
20 M. Shiraiwa, M. Ammann, T. Koop and U. Pöschl, *Proc. Natl. Acad. Sci. U. S. A.*, 2011, **108**, 11003–11008.
21 M. Kuwata and S. T. Martin, *Proc. Natl. Acad. Sci. U. S. A.*, 2012, **109**, 17354–17359.
22 S. Zhou, M. Shiraiwa, R. D. McWhinney, U. Pöschl and J. P. D. Abbatt, *Faraday Discuss.*, 2013, **165**, 391–406.
23 P. M. Medeiros and B. R. T. Simoneit, *Environ. Sci. Technol.*, 2008, **42**, 8310–8316.
24 R. Criegee, *Angew. Chem., Int. Ed.*, 1975, **14**, 745–752.
25 S. S. Steimer, U. K. Krieger, Y. F. Te, D. M. Lienhard, A. J. Huisman, B. P. Luo, M. Ammann and T. Peter, *Atmos. Meas. Tech.*, 2015, **8**, 2397–2408.
26 S. S. Steimer, M. Lampimäki, E. Coz, G. Grzinic and M. Ammann, *Atmos. Chem. Phys.*, 2014, **14**, 10761–10772.
27 M. Shiraiwa, C. Pfrang and U. Pöschl, *Atmos. Chem. Phys.*, 2010, **10**, 3673–3691.
28 U. Pöschl, Y. Rudich and M. Ammann, *Atmos. Chem. Phys.*, 2007, **7**, 5989–6023.
29 D. M. Murphy and D. W. Fahey, *Anal. Chem.*, 1987, **59**, 2753–2759.
30 D. O. Cooney, S.-S. Kim and E. James Davis, *Chem. Eng. Sci.*, 1974, **29**, 1731–1738.
31 M. Ammann, U. Pöschl and Y. Rudich, *Phys. Chem. Chem. Phys.*, 2003, **5**, 351–356.
32 J. Staehelin and J. Hoigne, *Environ. Sci. Technol.*, 1982, **16**, 676–681.
33 M.-T. Lee, M. A. Brown, S. Kato, A. Kleibert, A. Türler and M. Ammann, *J. Phys. Chem. A*, 2015, **119**, 4600–4608.
34 M. Ammann, R. A. Cox, J. N. Crowley, M. E. Jenkin, A. Mellouki, M. J. Rossi, J. Troe and T. J. Wallington, *Atmos. Chem. Phys.*, 2013, **13**, 8045–8228.
35 U. Pöschl, T. Letzel, C. Schauer and R. Niessner, *J. Phys. Chem. A*, 2001, **105**, 4029–4041.
36 N.-O. A. Kwamena, J. A. Thornton and J. P. D. Abbatt, *J. Phys. Chem. A*, 2004, **108**, 11626–11634.
37 N. O. A. Kwamena, M. G. Staikova, D. J. Donaldson, I. J. George and J. P. D. Abbatt, *J. Phys. Chem. A*, 2007, **111**, 11050–11058.
38 J. N. Crowley, M. Ammann, R. A. Cox, R. G. Hynes, M. E. Jenkin, A. Mellouki, M. J. Rossi, J. Troe and T. J. Wallington, *Atmos. Chem. Phys.*, 2010, **10**, 9059–9223.
39 W. L. Chameides, *J. Geophys. Res.*, 1984, **89**, 4739–4755.
40 S. E. Schwartz and J. E. Freiberg, *Atmos. Environ.*, 1981, **15**, 1129–1144.
41 A. K. Biń, *Ozone: Sci. Eng.*, 2006, **28**, 67–75.
42 R. Sander, *Atmos. Chem. Phys.*, 2015, **15**, 4399–4981.
43 J. Hoigne and H. Bader, *Water Res.*, 1983, **17**, 173–183.
44 S. D. Razumovskii and G. E. Zaikov, *Usp. Khim.*, 1980, **49**, 2344–2376.
45 J. Zahardis and G. A. Petrucci, *Atmos. Chem. Phys.*, 2007, **7**, 1237–1274.
46 M. Shiraiwa, Y. Sosedova, A. Rouvière, H. Yang, Y. Y. Zhang, J. P. D. Abbatt, M. Ammann and U. Pöschl, *Nat. Chem.*, 2011, **3**, 291–295.
47 M. Ammann and U. Pöschl, *Atmos. Chem. Phys.*, 2007, **7**, 6025–6045.